Study on the Periodic Flows in a Rectangular Container Under a Background Rotation

Yong Kweon Suh*, Jae Hyun Park
School of Mechanical and Industrial System Engineering, Dong-A University, 840 Hadan-dong, Saha-gu, Pusan 604-714, Korea
Sung Kyun Kim, Young Rak Son
School of Mechanical Engineering, KunKook University, Whayang-dong, Kwangjin-gu, Seoul 143-701, Korea

We present numerical and experimental results of the periodic flows inside a rectangular container under a background rotation. In numerical computation, a parallel-computation technique with MPI is implemented. Flow visualization and PIV measurement are also performed to obtain velocity fields at the free surface. Through a series of numerical and experimental works, we aim to clarify the fundamental reasons of discrepancy between the two-dimensional computation and the experimental measurement, which was detected in the previous study for the same flow model. Specifically, we check if the various assumptions prerequisite for the validity of the classical Ekman pumping law are satisfied for periodic flows under a background rotation.

Key Words : Periodic Flows, Background Rotation, Ekman Pumping, Rectangular Container

1. Introduction

In this study we present the results of numerical as well as experimental study on the periodic flows in a rectangular container which rotationally oscillates under a background rotation. For the same flow model, Suh and Kim (1998), Suh et al.(2000) conducted two-dimensional computation with a proposed Ekman pumping model and compared the results with the flow visualization. In their study the primary conclusion is that at low Rossby numbers the two results agree well with each other, whereas at the Rossby number 0.3 significant discrepancy exists.

On the other hand, when the proposed Ekman pumping law was applied to a simple spin-up flow inside a rectangular container (Suh, 1994, 2003; Suh and Choi, 2002) pioneered by van Heijst et al.(1990), the agreement was satisfactory even at relatively high Rossby numbers. This then indicates that there must be some physical explanation for the difference between the two flow models associated with such discrepancy. The main purpose of this study is to find, if any, what may cause such discrepancy in the periodic flows.

Compared with simple spin-up flows inside a circular or rectangular container, flows driven by a periodic forcing inside a circular container (Hart, 1990) or a rectangular container (Suh et al., 1998, 2000) provide persistent flows which are pertinent in real oceans or atmospheres; the periodic forcing mimics, for instance, winds over oceans whose directions are periodically changed.

In this study we conduct three-dimensional computation and flow-visualization experiment for the water flow inside a rectangular container of the horizontal aspect ratio 2. The main pur-

* Corresponding Author,
E-mail : yksuh@mail.donga.ac.kr
TEL : +82-51-200-7648; **FAX** : +82-51-200-7656
School of Mechanical and Industrial System Engineering, Dong-A University, 840 Hadan-dong, Saha-gu, Pusan 604-714, Korea. (Manuscript **Received** April 7, 2003; **Revised** January 12, 2004)

pose of this study is to capture fundamental reasons for the early-reported discrepancy between the two-dimensional computation and the flow visualization. The ultimate goal of the series of our studies is to develop an improved Ekman pumping model.

2. Flow Model and Governing Equations

2.1 Flow model

Figure 1 shows the flow model and the coordinate system. The container rotates around the vertical axis $x^*=aL/2$, $y^*=L/2$ with an angular velocity $\Omega(t)$ which is composed of a constant value Ω_b (background rotation) and a periodic one; $\Omega=\Omega_b+\Omega_a \sin \omega^* t^*$, see Fig. 2. The fluid depth is denoted by H, the width of the container by L, and the length by aL where a corresponds to the horizontal aspect ratio. In this study we confine ourselves to $a=2$.

2.2 Governing equations

Scaling the velocities by $L\Omega_a$, the time by $1/\Omega_a$, the spatial coordinates by L, and the pressure by $\rho L^2\Omega_a\Omega_b$, we can obtain the nondimensional governing equations as follows.

$$\frac{\partial u}{\partial x}+\frac{\partial v}{\partial y}+\frac{\partial w}{\partial z}=0 \tag{1}$$

$$\frac{\partial u}{\partial t}+u\frac{\partial u}{\partial x}+v\frac{\partial u}{\partial y}+w\frac{\partial u}{\partial z}-2\left(\frac{1}{\varepsilon}+f\right)v = -\frac{1}{\varepsilon}\frac{\partial p}{\partial x}+\frac{1}{Re}\nabla^2 u+y\frac{df}{dt} \tag{2a}$$

$$\frac{\partial v}{\partial t}+u\frac{\partial v}{\partial x}+v\frac{\partial v}{\partial y}+w\frac{\partial v}{\partial z}+2\left(\frac{1}{\varepsilon}+f\right)u = -\frac{1}{\varepsilon}\frac{\partial p}{\partial y}+\frac{1}{Re}\nabla^2 v-x\frac{df}{dt} \tag{2b}$$

$$\frac{\partial w}{\partial t}+u\frac{\partial w}{\partial x}+v\frac{\partial w}{\partial y}+w\frac{\partial w}{\partial z} = -\frac{1}{\varepsilon}\frac{\partial p}{\partial z}+\frac{1}{Re}\nabla^2 w \tag{2c}$$

Here t is the dimensionless time, x, y, z, are dimensionless coordinates corotating with the container, and u, v, w are dimensionless velocity components along the $x-$, $y-$, and $z-$ directions, respectively. The function $f=\sin wt$ represents the oscillatory component of the table's angular velocity and its derivative with respect to the time produces the body forces, the last terms of Eq. (2a) and (2b). Dimensionless parameters appearing in the above formulations and the subsequent analysis are

$$Re=\frac{L^2\Omega_a}{\nu},\quad \varepsilon=\frac{\Omega_a}{\Omega_b},\quad \omega=\frac{\omega^*}{\Omega_a},\quad h=\frac{H}{L} \tag{3}$$

where Re is the Reynolds number, ε the Rossby number, ω the dimensionless angular velocity of the periodic rotational motion of the table and h the dimensionless liquid depth.

We define the kinetic energy $E(z, t)$ averaged over a horizontal plane of the domain as

$$E(z, t)=\frac{1}{A}\int(u^2+v^2)\,dxdy \tag{4}$$

for use in the analysis. The area A of the horizontal plane is 2 in this study.

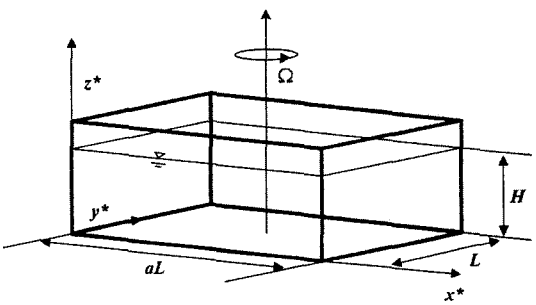

Fig. 1 Schematic diagram of the model basin

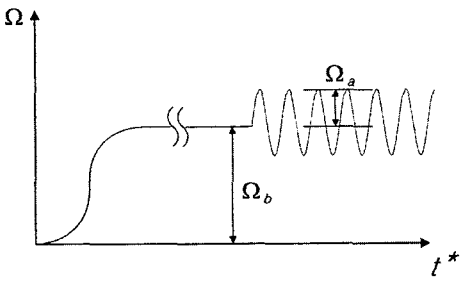

Fig. 2 Angular velocity of the turn table

3. Numerical and Experimental Methods

3.1 Numerical methods

The spatial derivatives in the governing equations are discretized with a central difference scheme and the time derivative by the explicit Euler method. Depending on Re, the time step $\triangle t$ was adjusted within the range $0.001 \sim 0.005$. For the efficiency of the calculation in the parallel architecture, the pressure equation was solved by using PCGM (pre-conditioned conjugate gradient method) together with the D-ILU (diagonal-incomplete LU) as a pre-conditioner.

No-slip and impermeable conditions are applied as boundary conditions on the solid walls, and no-stress condition on the free surface. The pressure conditions on the solid boundaries are given by applying these conditions to the Eqs. (2a) ~ (2c) for the corresponding boundaries, and that on the free surface is maintained 0.

We conducted the numerical computations for three cases as shown in Table 1. The number of grids for all cases is $I \times I \times K = 150 \times 75 \times 30$.

3.2 Experimental methods

Figure 3 shows the experimental apparatus. The horizontal dimension of the rectangular container is 0.3[m]×0.15[m]. The angular speed of the table is adjusted by a servo motor. Adjustment of the table's speed is as shown in Fig. 2. In this study the angular speeds are; $\Omega_b = 3.29$ [rpm], $\Omega_a = 0.663$[rpm] for the case 1, $\Omega_b = 5$ [rpm], $\Omega_a = 1$[rpm] for the case 2 and $\Omega_b = 3.34$ [rpm], $\Omega_a = 1$[rpm] for the case 3. The angular speed of the modulation for the table's rotational oscillation is $\omega^* = 0.263$[rpm] for the case 1 and $\omega^* = 0.4$[rpm] for the case 2 and 3.

Particles used in the flow visualization are acrylic powders with the average diameter 0.35 mm and the specific gravity 1.18. Since the flow is slowly decaying in time (almost steady), the size of the particles for the PIV analysis is thought to be reasonably selected considering the container size. A CCD camera (made by Lavision Co. with maximum resolution 1208 * 1024) is used to record the particle motions on the free surface. The software used for the PIV analysis is 'Window with CBC'. The time interval of the two images used in the PIV computation is 1/7 sec. Since the flow evolution is slow, this time interval is short enough for the result to represent the instantaneous velocity field.

Table 1 Parametric values for each computational case

case	1	2	3
Re	1548	2356	2356
ω	0.4	0.4	0.4
ε	0.2	0.2	0.3
h	0.4	0.4	0.4

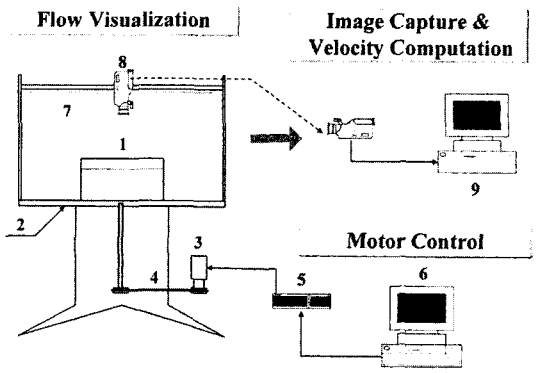

1. Rectangular Container 2. Turntable
3. Servo Motor 4. Timing Belt
5. Servo Motor Controller 6. Motor Control PC
7. Fluorescent Light 8. CCD Camera
9. Host Computer & Image Grabber

Fig. 3 Schematic diagram of the experimental apparatus

4. Results and Discussions

4.1 Periodic nature of the flows and the horizontal flow-patterns

At low Reynolds numbers the flow remains periodic in time. Shown in Fig. 4 is the temporal behavior of $E(h, t)$, the spatially averaged kinetic energy of the free-surface flows. These are obtained from the numerical computation. It is seen that the flows become periodic after a few periods of initial transient state. All the results

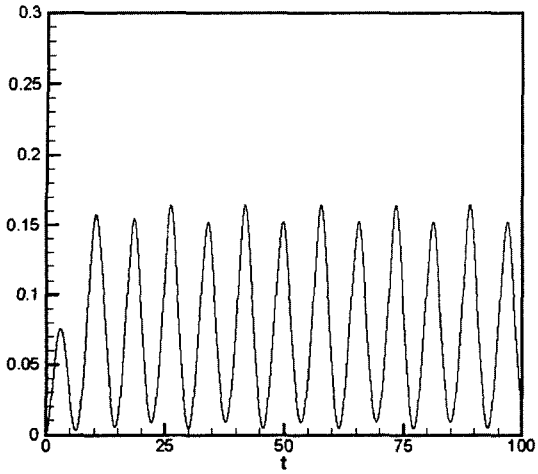

(a) Case 1 (Re=1548, ε=0.2)

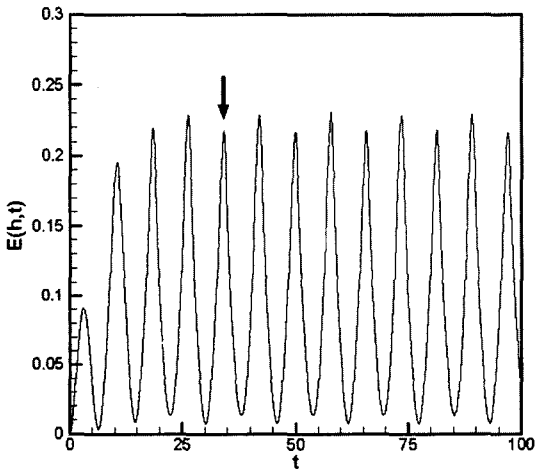

(b) Case 2 (Re=2356, ε=0.2)

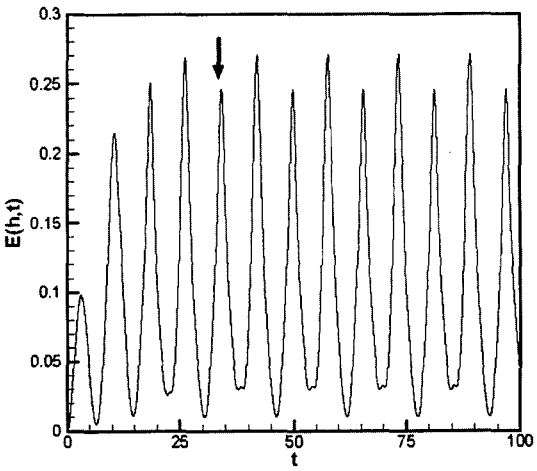

(c) Case 3 (Re=2356, ε=0.3)

Fig. 4 Time history of the spatially averaged kinetic energy

shown in this paper are taken during this periodic state.

Comparing the case 1 and 2, we can see that increase of Re evidently results in a stronger flow, as is usual. Increase of ε also results in a stronger flow as seen by comparing the case 2 and 3. This can be explained by using the discussions and formulations given by Suh and Choi (2003). According to the classical Ekman pumping law, the Ekman pumping velocity is proportional to $\sqrt{\varepsilon/Re}$. When this is substituted into the vorticity equation, it results in a vorticity-dynamical equation in which $d\zeta/dt$ is proportional to $-\zeta/\sqrt{Re\,\varepsilon}$ under the restriction of small ε. Therefore, when either Re or ε is increased the damping coefficient $1/\sqrt{Re\,\varepsilon}$ decreases, and thus the fluid motion becomes stronger as shown in Fig. 4.

We also compared the kinetic energy averaged over each horizontal plane and found that the kinetic energy at the free surface is the smallest but difference between the value at each level is insignificant.

Figure 5 shows velocity vectors at the free surface at four instants for the case 2. The first frame is taken when the kinetic energy becomes momentarily maximum after two forcing periods as indicated by a downward arrow in Fig. 4(b). The subsequent frames are taken at a constant interval of time $T/4$. First of all we note that the numerical and experimental results agree very well with each other. This indicates that the overall methods used in our three-dimensional computation are relevant and trustworthy. Next, we focus our attention on the evolution of the flow patterns. If no Ekman pumping effects are present and if there occurs no boundary-layer separation from the side walls, the flow must be purely inertial. In this ideal case, at $t=2T$ (or 3 T, 4T, $\cdots$) the fluid must be motionless because at this time the perturbed angular speed of the table $f=\sin \omega t$ is zero. Similarly the fluid must rotate in the clockwise direction (anticyclonic) with maximum kinetic energy at $t=2.25T$, become again stagnant at $t=2.5T$, and rotate in the counterclockwise direction (cyclonic) with maximum kinetic energy at $t=2.75T$. In Fig. 5,

however, the corresponding times are roughly $0.073T$ (or 26° out of 360°) ahead of this ideal case. This is attributed to the damping caused mostly by the Ekman pumping from the bottom boundary layer.

Figure 6 shows results for the case 3 in which only the Rossby number is increased. Here the two-dimensional numerical results are obtained

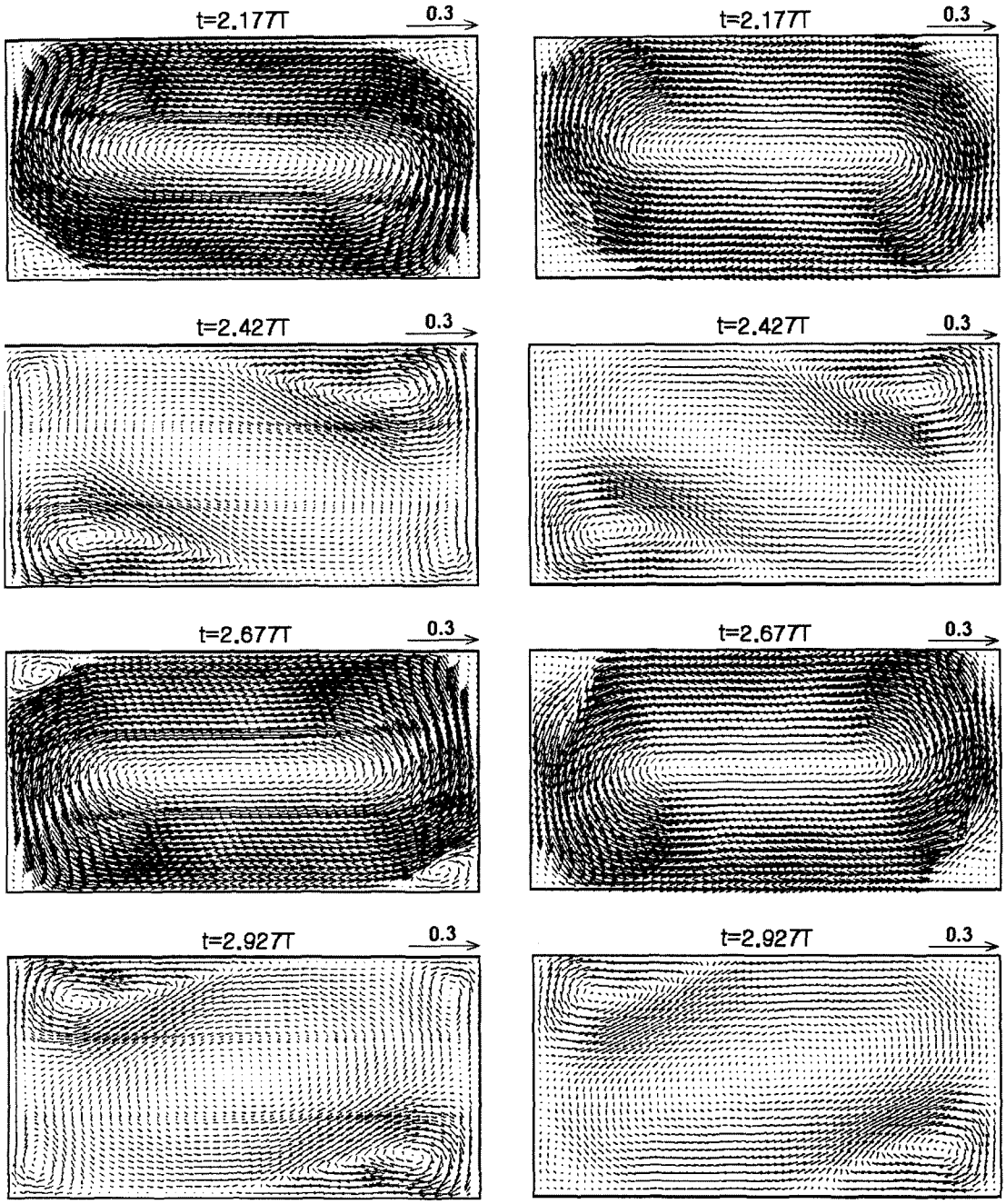

(a) Numerical result (b) PIV result

Fig. 5 Velocity vectors on the free surface for the case 2

by using the Ekman pumping model suggested by Suh and Choi (2003). We can see that at higher Rossby numbers, especially the coner vortices become stronger, this is consistent with the results shown in Fig. 4 and the reason for the higher kinetic energy at higher Rossby number is now attributed to these coner vortices. As explained previously this is due to decrease of the damping coefficient at higher Rossby number. On the other hands, the flow motion is stronger in two-dimensional numerical results compared with three-dimensional numerical and experimental results. We can infer from these results that the 2-D equations with the Ekman pumping model cannot reproduce the actual flow field exactly. The significant discrepancy between the 2-D numerical result with the experimental result is remarkable because $\varepsilon=0.3$ was categorized as the parameter value at which the 2-D numerical results were in good agreement with the experimental results for the case of spin-up flows (see e.g. Suh and Choi, 2003). Therefore we need further studies to clarify the basic mechanism under which such discrepancy is observed.

Figure 7 shows the streamlines at four different horizontal planes for the case 1 at two instants of time. This figure reveals that the flow patterns are almost invariant of the vertical position, which was also confirmed from the time history of the kinetic energy at different horizontal planes. This supports the preassumption necessary for the classical Ekman pumping laws.

4.2 Vertical distribution of the velocity components

Figure 8 shows the velocity vectors at four in-

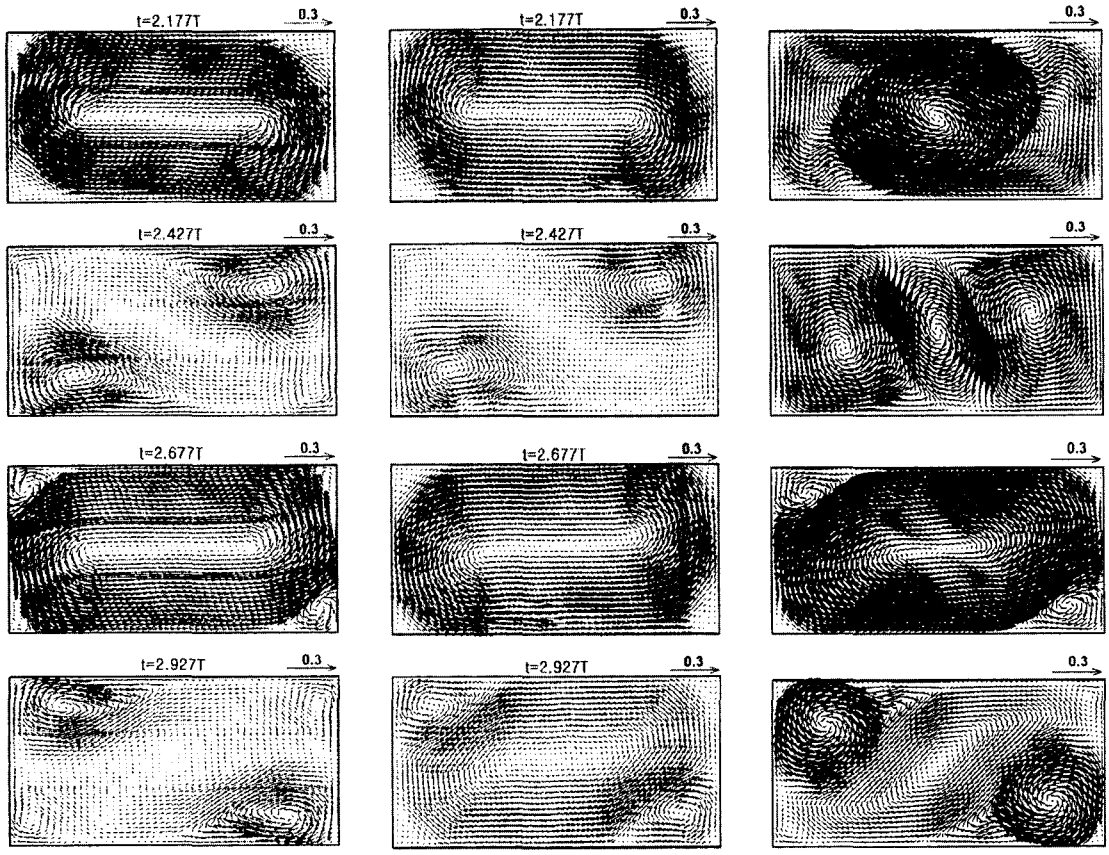

(a) 3-D numerical result (b) PIV result (c) 2-D numerical result

Fig. 6 Velocity vectors on the free surface for the case 3

stants at the vertical plane $y=0.5$ for the case 3. This figure also reveals that the flow patterns are almost independent of the vertical positions of the plane.

The fact that the horizontal velocity-components (u, v) are independent of the vertical positions does not necessarily mean that the vertical velocity component w is a linear function of z as might be seen from the continuity Eq. (1). Fig. 9 shows time history of the vertical distributions of the velocity component w at $y=0.75$ and at three x-coordinates for a very short duration. During this time interval, the primary flow is cyclonic in the central region and anti-cyclonic near the corners, Fig. 6. Therefore following the Ekman pumping law, the fluid is

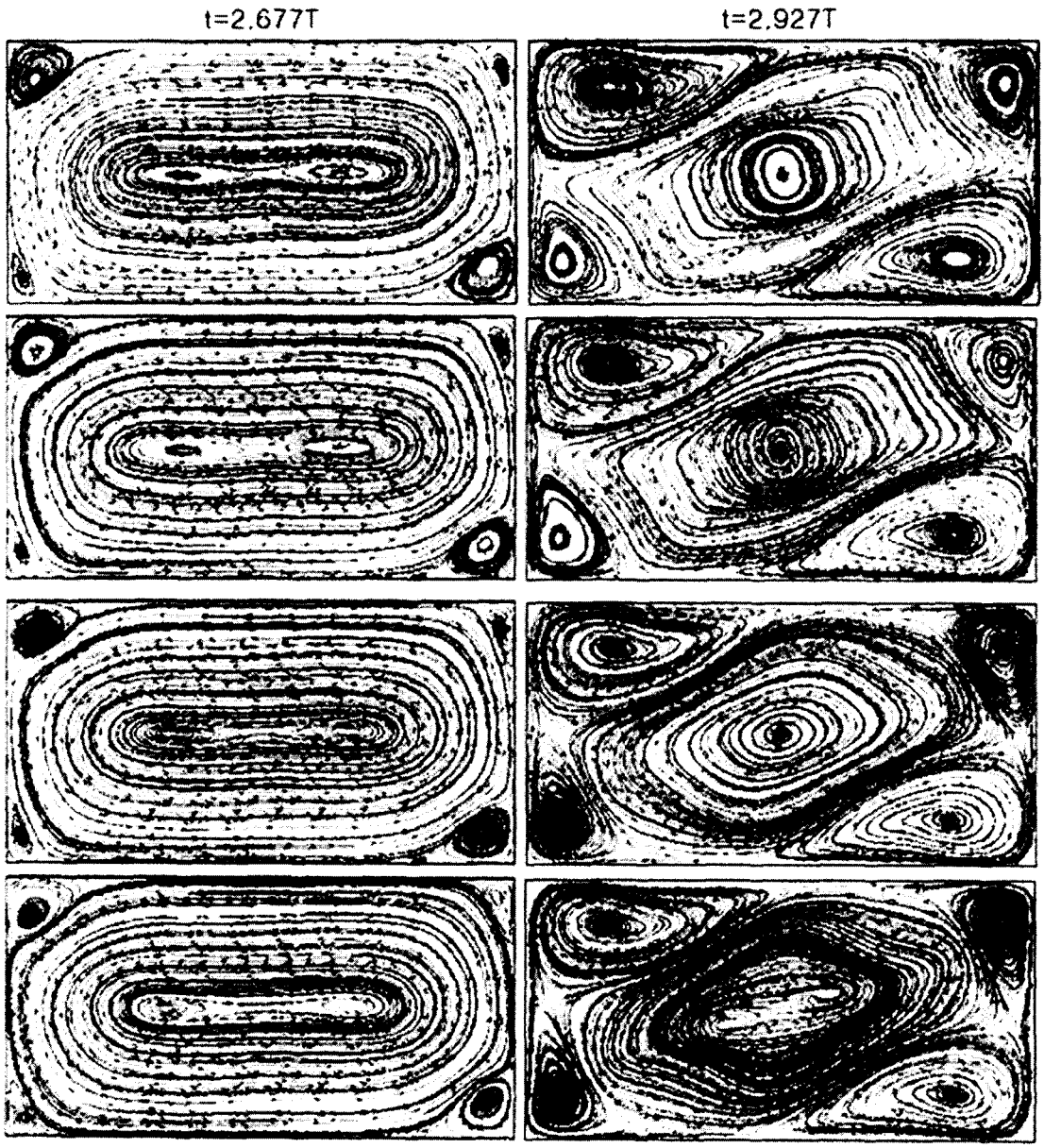

Fig. 7 Streamline plots on the horizontal planes at $t=2.677T$ for the case 1 (left frames) and $t=2.927$ for the case 2 (right frames); $z=h$, $3h/4$. $2h/4$ and $h/4$ (from top to bottom)

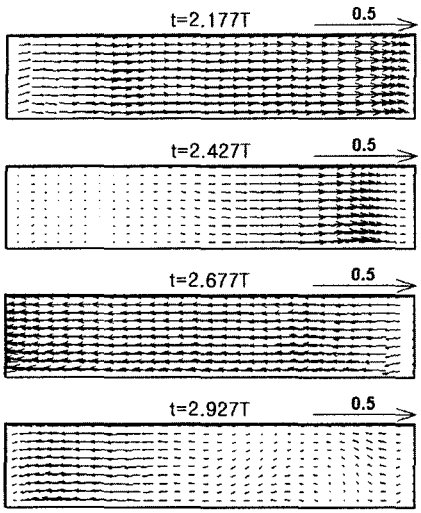

Fig. 8 Velocity vector plots on the vertical plane $y=0.5$ for the case 3

predicted to be pumped from the bottom boundary-layer ($w>0$; Fig. 9(b)) in the central region, and sucked ($w<0$; Fig. 9(a) and 9(c)) in the corner regions, and these predictions are quite right almost all over the regions. However the distributions at $x=0.016$ and at $x=1$ are significantly nonlinear and more importantly the distribution changes very rapidly with time in the central region.

Figure 10 shows time history of the vertical velocity component at several fixed points in the space. It also exhibits a very rapid temporal change of the vertical velocity component at the central region.

These figures clearly indicate that one of the pre-assumptions for the classical Ekman pumping law, that is the vertical velocity should be proportional to $(h-z)$, is not satisfied. Therefore we need somehow to admit the nonlinear distribution of the vertical-velocity component for an efficient two-dimensional approximation of the rotating flows at high Reynolds numbers and high Rossby numbers.

5. Conclusions

We can summarize our important findings in this study as follows.

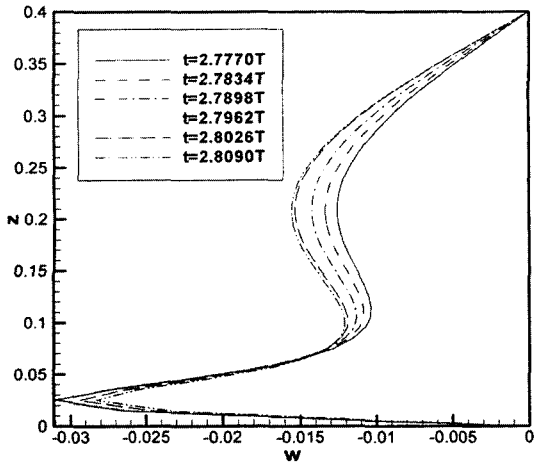

(a) $x=0.016$, $y=0.75$

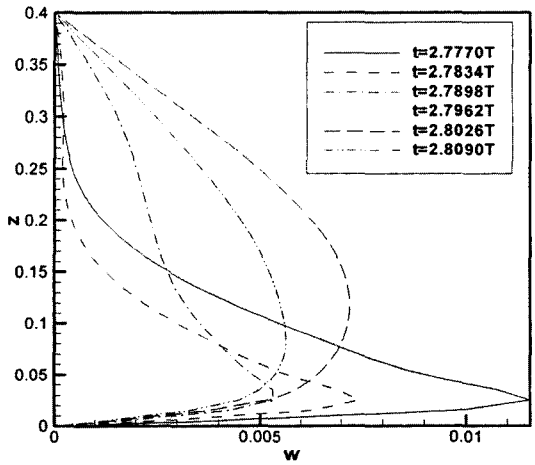

(b) $x=1.0$, $y=0.75$

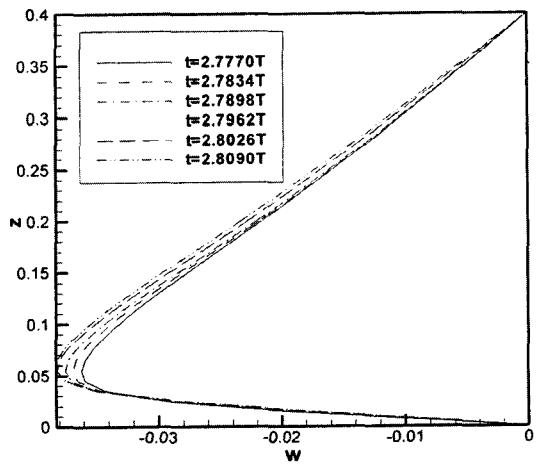

(c) $x=1.984$, $y=0.75$

Fig. 9 Distribution of the vertical velocity w at three locations shown for the case 3 at six instants of time

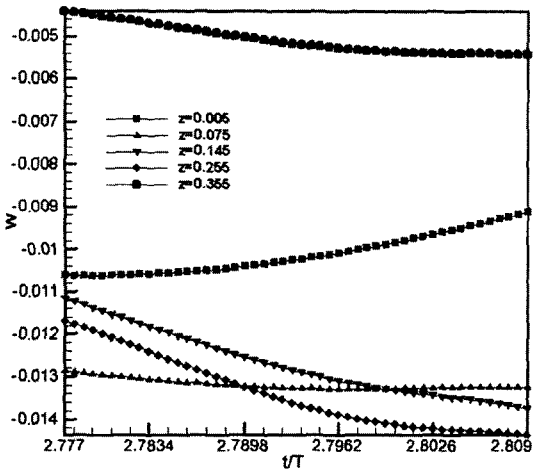

(a) $x=0.016$, $y=0.75$

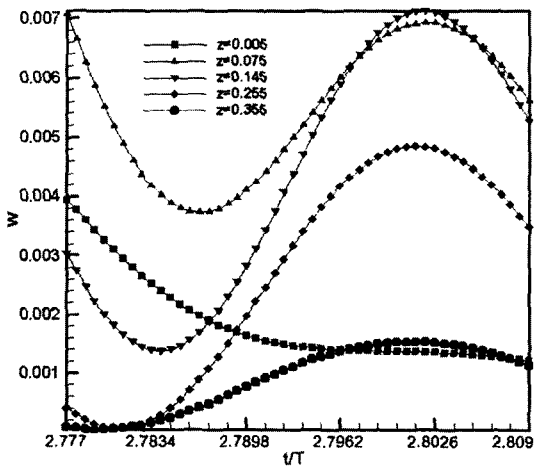

(b) $x=1.0$, $y=0.75$

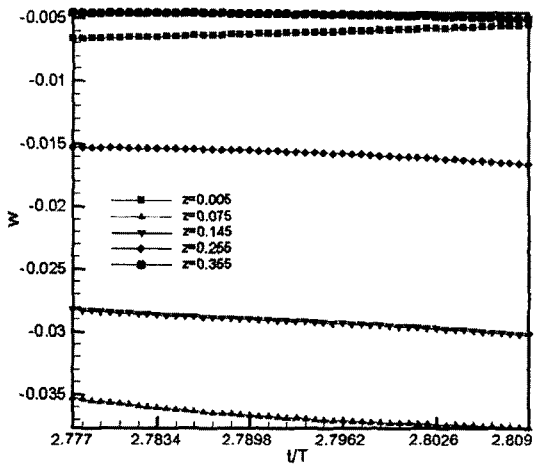

(c) $x=1.984$, $y=0.75$

Fig. 10 Time history of the vertical velocity w for the case 3

(1) In general the flows become stronger as the Reynolds number and the Rossby number increase.

(2) The three-dimensional numerical results are almost in a perfect agreement with the experimental ones, whereas the two-dimensional numerical results show a significant discrepancy.

(3) Except for the bottom Ekman boundary-layer, the flow patterns on the horizontal planes are almost unchanged for different vertical positions, and this satisfies the assumption of the classical Ekman pumping law.

(4) The vertical distribution of the vertical velocity component is no longer linear in the central region, and moreover its variation in time is significant, which is not consistent with the assumption underlying the classical Ekman pumping law, which must be considered to develop an improved Ekman pumping model.

Acknowledgment

This study is supported from the Korea Science and Engineering Foundation via the grant No. R01-2000-00290.

References

Hart, J. E., 1990, "On Oscillatory Flow over Topography in a Rotating Flow," *J. Fluid Mech.*, Vol. 214, pp. 437~454.

Suh, Y. K. and Kim, Y. K., 1998, "Study on Fluids in a Rectangular Container Subjected to a Background Rotation with a Rotational Oscillation," *Proc. KSME 1998 Fall Annual Meeting B*, pp. 869~875.

Suh, Y. K. and Choi, Y. H., 2002, "Study on the Spin-up of Fluid in a Rectangular Container Using Ekman Pumping Models," *J. Fluid Mech.*, Vol. 458, pp. 103~132.

Suh, Y. K., 1994, "Numerical Study on Two-Dimensional Spin-up in a Rectangle," *Phys. Fluids*, Vol. 6, No. 7, pp. 2333~2344.

Suh, Y. K., 2003, "Multi-Frame MQD-PIV," *KSME Int.*, Vol. 17, No. 10, pp. 1552~1562.

Suh, Y. K., Choi, Y. H., Kim, S. K. and Lee, D. Y., 2000, "Study on Fluid in a Rectangular

Container Subjected to a Background Rotation with a Rotational Oscillation Using PIV System," *Trans. KSME (B)*, Vol. 24, No. 6, pp. 845~851.

van Heijst, G. J. F., Davies, P. A. and Davies, R. G., 1990, "Spin-up in a Rectangular Containers," *Phys. Fluids*, Vol. 2, No. 2, pp. 150~159.